



City Research Online

City, University of London Institutional Repository

Citation: Mergos, P. E. (2024). Benchmark problems in optimum structural design of 3D reinforced concrete frames. *Journal of Building Engineering*, 91, 109554. doi: 10.1016/j.jobe.2024.109554

This is the accepted version of the paper.

This version of the publication may differ from the final published version.

Permanent repository link: <https://openaccess.city.ac.uk/id/eprint/32857/>

Link to published version: <https://doi.org/10.1016/j.jobe.2024.109554>

Copyright: City Research Online aims to make research outputs of City, University of London available to a wider audience. Copyright and Moral Rights remain with the author(s) and/or copyright holders. URLs from City Research Online may be freely distributed and linked to.

Reuse: Copies of full items can be used for personal research or study, educational, or not-for-profit purposes without prior permission or charge. Provided that the authors, title and full bibliographic details are credited, a hyperlink and/or URL is given for the original metadata page and the content is not changed in any way.

Benchmark problems in optimum structural design of 3D reinforced concrete frames

Panagiotis E. Mergos ^{a,*}

^a *Department of Civil Engineering, City, University of London, London EC1V 0HB, UK*

Abstract.

Benchmarking goes hand in hand with the development and establishment of efficient and robust optimization methodologies in various scientific fields. Nevertheless, benchmark problems, with known global optima, are currently missing in the optimum structural design of reinforced concrete (RC) frames. In the present study, for first time, benchmark case studies in the optimum design of RC frames are presented. The aim is that these benchmarks are used for the calibration, tuning, improvement and development of optimization algorithms to address the efficient design of concrete frames. More particularly, six three-dimensional concrete building frames are optimally designed to Eurocodes. First, exhaustive search is conducted to identify the global optimum solutions and Pareto fronts. Useful conclusions are also made with respect to the properties of the optimal solutions. Moreover, all candidate designs results are provided in an accompanying file so that they can be used in future optimization studies. Next, the performance of several well-known, single- and multi-objective optimization algorithms is assessed against the global optima to examine their efficiency and applicability in this class of optimization problems. Closing, the need for further and larger in scale benchmark case studies in the optimum design of concrete frames is emphasized.

Keywords: Reinforced concrete; Benchmarks; Structural; Optimization; Metaheuristics; Eurocodes

1 Introduction

Reinforced concrete (RC) structures are ubiquitous in the built environment. At the same time, they are related to high financial costs and environmental impacts [1-5]. Therefore, efficient design of concrete structures plays a vital role in sustainable development worldwide [1-5]. RC frames are widely met in concrete structures. They represent rather complex structural systems with multiple and nonlinear interdependencies that prohibit their optimum design by manual trial and error procedures [6-7]. Hence, the application of automated optimization algorithms is generally recommended in the sustainable design of RC frames [6-8].

Scientific research focussing on automated optimum design of RC frames initiated several decades ago [6]. Today, there exists a large number of studies in this area. However, the vast majority of these studies deal with either single structural members (i.e. slabs, beams, columns)

* Corresponding author. Panagiotis E. Mergos, Senior Lecturer in Structural Engineering, Research Centre for Civil Engineering Structures, City, University of London, London, EC1V 0HB, UK.
E-mail address: panagiotis.mergos.1@city.ac.uk, Tel. 0044 (0) 207040 8417

(e.g. [4, 9-11]), or planar RC frames (e.g. [12-17]). The author has identified solely the following studies addressing the optimum design of three-dimensional concrete frames: [7, 18-28]. The rather limited number of these studies can be attributed to the additional complexity and computational cost involved when designing 3D concrete frames.

All previous research efforts, investigate the application of newly developed, improved or even existing optimization methods to the structural design of RC frames. The performance of the adopted optimization methods is compared with other methods in literature and the superiority of the former with respect to the latter is, typically, concluded. However, the global optimum solution of the examined RC frames is not known. Therefore, the efficiency of the optimization algorithms cannot be concluded in absolute terms but only with respect to other methodologies. Furthermore, the computational frameworks developed or applied for the optimum design of the RC frames are, typically, not shared with readers or fully described in papers. Consequently, the results of these optimization studies cannot be reproduced by other researchers for verification purposes and future comparisons with new algorithms.

The previous discussion hints at the lack of established benchmarks in the optimum structural design of real-world 3D concrete frames. This is despite the fact that benchmarking goes hand in hand with the development of optimization techniques in the various scientific fields. As a matter of fact, from its very beginning in the 1960s, evolutionary computation was accompanied by benchmarking studies [29]. Some of the very first benchmarks, such as the Rosenbrock's [30] and Rastrigin's functions [31] (Fig. 1), are still widely used to calibrate optimization algorithms. Nowadays, apart from benchmark suites consisting of purely mathematical functions (e.g. [32-35]), there exists a significant number of benchmark case studies related to real-world optimization tasks (e.g. [36-39]). At the same time, it is well-known that the performance of optimization algorithms cannot be generalized to other problem classes or fields [29]. Explaining the no free lunch theorem, Haftka [40] states that improving an algorithm for a class of problems is likely to make it perform more poorly for other

problems. The previous observations highlight the need for optimization benchmarks for each scientific field or class of problems.

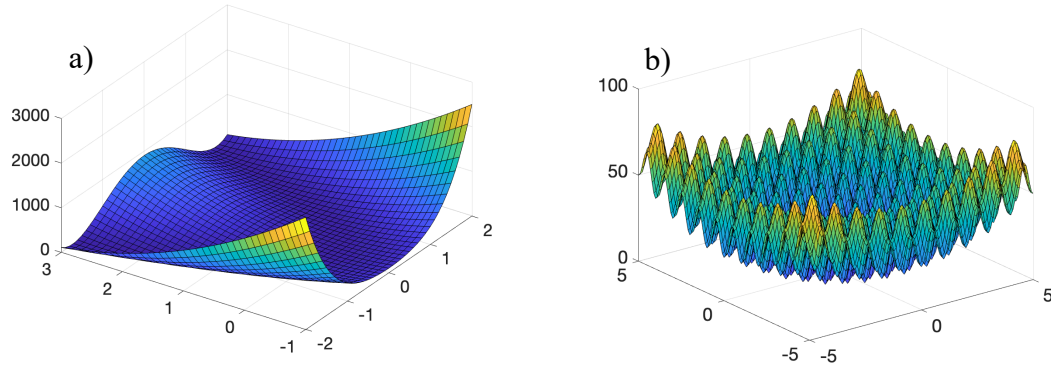


Fig. 1: Benchmark optimization functions: a) Rosebrock's function; b) Rastrigin's function

In the following of this study, a suite of six small-scale benchmark case studies in the optimum structural design of RC building frames is presented. This is the first time that benchmark problems are developed for this optimization task. All building frames are designed in accordance with the prescriptions and design constraints of Eurocode 2 [41] and Eurocode 8 [42] for ductility class low. The benchmark problems are developed for both single- and multi-objective optimization frameworks. The main aim here is that the benchmarks are used in the future calibration, tuning, improvement and development of direct search methods and evolutionary optimization algorithms to address this class of optimization problems. In all benchmark case studies, exhaustive search is first applied and thereby global optima are established with certainty. Furthermore, the results of all candidate design solutions are provided in an accompanying file of this manuscript so that they can be employed in future optimization studies. In addition to exhaustive search, several existing single- and multi-objective optimization algorithms are applied to optimize the examined RC frames. The performances of these algorithms are analysed and compared in terms of actual errors with respect to the global optimum solutions and thereby objective conclusions are made with respect to the efficiency of existing optimization algorithms in structural design of RC frames.

2 Optimization framework

The present optimization framework aims at minimizing the upfront economic cost or embodied carbon of 3D RC frames so that they, at least, satisfy the minimum structural performance requirements set by modern structural design guidelines, such as the Eurocodes. This approach aligns well with standard engineering practice and therefore is expected to have a direct and significant impact on sustainable construction. Alternatively, RC frames can be optimally designed to maximize structural performance or minimize structural damage, measured by appropriate indicators such as interstorey drifts and damage indices, for given available resources. Furthermore, a multi-objective optimization approach can be adopted where the best trade-off solutions between structural damage and upfront costs for the RC frames will be identified for these conflicting objectives. Last but not least, RC frames may be designed for minimum life-cycle cost that includes both initial costs and costs related to structural damages and deterioration during the life cycle of the structures.

More particularly, the optimization framework of the current study examines the optimal sizing of cross-sections in RC frames to minimize material quantities, environmental impacts or economic costs. In this endeavor, frame geometry, external loads, material properties and boundary conditions are assumed pre-specified and fixed. Therefore, the vector of design variables consists solely of the concrete cross-sections allocated to various groups of RC members in the frames. Furthermore, to conform with standard construction practice, cross-sections are obtained from user-specified, discrete lists of available cross sections. The afore-described optimization problem is formulated as:

$$\begin{aligned} \text{Minimize:} & \quad F_1(\mathbf{x}), F_2(\mathbf{x}), \dots, F_n(\mathbf{x}) \\ \text{Subject to:} & \quad g_j(\mathbf{x}) \leq 0, \quad j = 1 \text{ to } m \\ \text{Where:} & \quad \mathbf{x} = (x_1, x_2, \dots, x_d) \\ & \quad x_i \in \mathbf{D}_i = (1, 2, \dots, k_i), \quad i = 1 \text{ to } d \end{aligned} \tag{1}$$

In this formulation, $F_l(\mathbf{x})$ ($l = 1$ to n) are the n objective functions to be minimized, and \mathbf{x} is the design variables vector that comprises of d independent variables x_i ($i = 1$ to d), representing concrete cross-sections, where d is the total number of member groups in the RC frames with potentially different cross-sections. The design variables x_i take values from integer values sets $\mathbf{D}_i = (1, 2, \dots, k_i)$ reflecting the positions of cross-sections in the corresponding lists of available sections and k_i is the total number of available cross-sections in the list for group i ($i = 1$ to d). In addition to the above, the solution must be subject to m number of constraints $g_j(\mathbf{x}) \leq 0$ ($j = 1$ to m). The penalty function approach is used in the present study to account for constraints violation.

The objective functions $F_l(\mathbf{x})$ ($l = 1$ to n) are calculated by the generic Eq. (2), where V_c (m^3) represents the total frame concrete volume and m_s (kg) stands for the total mass of the steel reinforcement accounting for both the longitudinal (flexural) bars and transversal (shear) links. In Eq. (2), f_{co} and f_{so} are the prices of concrete per unit volume and reinforcing steel per unit mass, respectively. By applying appropriate material unit prices, Eq. (2) may focus on material quantities, economic costs or even environmental impacts [4-5].

$$F_l(\mathbf{x}) = V_c(\mathbf{x}) \cdot f_{co} + m_s(\mathbf{x}) \cdot f_{so} \quad (2)$$

In Eq. (2), the concrete volume $V_c(\mathbf{x})$ is directly calculated by the member cross-sections of the design vector \mathbf{x} and frame geometry. Furthermore, for a given set of frame cross-sections (i.e. \mathbf{x} vector), the mass of steel reinforcement $m_s(\mathbf{x})$ is obtained by following standard structural analysis and design procedures. More particularly, in the present framework, the design guidelines of Eurocode 0 [43], Eurocode 2 [41] and Eurocode 8 [42] for low ductility class (DCL) are applied. To serve this goal, structural analysis and design are conducted with the aid of the well-established integrated structural analysis and design software SAP2000 [44] version 18. Interaction with SAP2000 is achieved via its Application Programming Interface

(API) and the use of a special-purpose application, namely STROLAB (STRuctural Optimization LABoratory), developed by the author [27] in MATLAB [45].

In more detail, structural analysis is first conducted, with the aid of SAP2000, for the various load cases (e.g. dead, live, wind, seismic) specified by the designer. Next, design action effects (i.e. bending moments, shear and axial forces) are calculated for the ultimate limit state (ULS) design load combinations prescribed by Eurocode 0 [43] for persistent, transient, accidental or seismic design situations. For the obtained design action effects, concrete beams and columns are designed for bending, shear and torsion at a number of cross-sections equally spaced along member lengths again with the aid of SAP2000 [44]. Eleven design sections are assumed for concrete beams and three for column members. Furthermore, it is assumed that the provided steel reinforcement areas match the required ones of the design sections and that these are extended till the neighbouring design sections of the same member with lower reinforcement demands. For simplicity, rectangular beam and square column sections are assumed herein with steel reinforcement arrangement as shown in Fig. 2. However, it is clarified that the optimization framework can address any geometry of cross-sections as long as they are introduced in the discrete lists of available cross-sections \mathbf{D}_i ($i = 1$ to d) of Eq. (1) and the calculation of required steel reinforcement is feasible for given design action effects.

Specifically, concrete beam sections are first designed for major bending to establish the required longitudinal reinforcement (i.e. $A_{s,top}$ and $A_{s,bot}$ in Fig. 2) assuming the simplified stress block of EC2 §3.1.7(3) [27, 41, 46]. Next, beams are designed for major shear employing the variable strut inclination method of EC2 [27, 41, 46] to establish the required shear reinforcement area (i.e. A_{sw}/s in Fig. 2). In addition, beams are designed for torsion to establish whether additional longitudinal and shear reinforcement is required [41, 46]. For column members, the longitudinal reinforcement area $A_{s,tot}$ (Fig. 2) of cross-sections is designed for combined axial load and biaxial bending moments effects (i.e. $N + M_x + M_y$) by ensuring that all action effects points are within the corresponding 3D axial force-biaxial bending moment

interaction surfaces and that utilization factors are close to unity [27, 46]. In addition, the required shear reinforcement is calculated in both horizontal directions (i.e. A_{swx} / s_x and A_{swy} / s_y in Fig. 2) employing similar procedures to beams [27, 46].

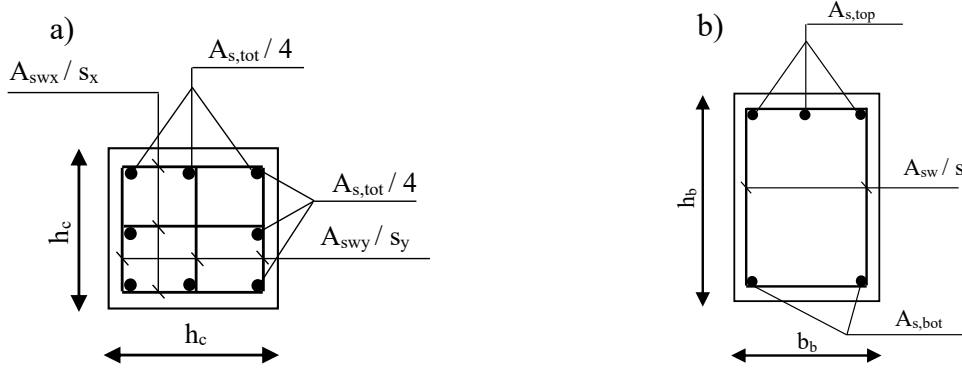


Fig. 2: Assumed concrete cross-sections and steel reinforcement configurations: a) columns; b) beams

The design constraints $g_j(\mathbf{x}) \leq 0$ ($j = 1$ to m) of the present optimization framework reflect the design checks required by Eurocode 2 [41] and Eurocode 8 (DCL) [42] to fulfil the ULS and SLS limit states. More specifically, a ULS design constraint is considered not to be met when the corresponding limit state check (i.e. bending, shear, torsion, deflections) cannot be satisfied by any allowable amount of steel reinforcement in the concrete sections. This approach is adopted herein since only concrete cross sections are treated as independent design variables. Following this approach, a constraint for the flexural and/or shear design at the ULS of a beam or column section is assumed not to be satisfied when the required flexural and/or shear reinforcement areas exceed the maximum permissible values. These constraints are written as below, where ρ_l and ρ_w are the required cross-section longitudinal and transverse steel reinforcement volumetric ratios respectively and $(\rho_{l,max} = 4\%)$ and $\rho_{w,max}$ their corresponding maximum permissible values according to Eurocodes and construction practice.

$$\rho_l - \rho_{l,max} \leq 0 \quad (3)$$

$$\rho_w - \rho_{w,max} \leq 0 \quad (4)$$

Moreover, a constraint for the design against shear and torsion at the ULS is considered violated when the combined shear and torsion effects at a concrete section exceed the maximum capacity of the concrete member diagonal compressive struts. These constraints are written in the following form, where V_{Ed} and T_{Ed} are the shear force and torsional moment demands, respectively, and $V_{Rd,max}$ and $T_{Rd,max}$ are the corresponding diagonal compression capacities for an angle of compression struts $\theta = 45^\circ$.

$$\frac{V_{Ed}}{V_{Rd,max}} + \frac{T_{Ed}}{T_{Rd,max}} - 1 \leq 0 \quad (5)$$

Regarding SLS, SAP2000 v18 does not explicitly check for deflections of concrete beams [46]. To check this limit state, the limiting span-to-depth ratio (L/d) approach is adopted in the present study [47]. The method guarantees that beam deflections do not exceed the span length divided by 250. Hence, a design constraint for beam deflections is assumed not to be fulfilled when the member span-to-depth ratio exceeds the corresponding permissible value $(L/d)_{max}$. This design constraint is expressed as:

$$\left(\frac{L}{d}\right) - \left(\frac{L}{d}\right)_{max} \leq 0 \quad (6)$$

Furthermore, for the purposes of seismic design, the SLS is verified by comparing inter-storey drift ratios demands IDR for the frequent earthquake against limit values IDR_{max} depending on the type of non-structural elements following the prescriptions of EC8 [42]. The latter constraints are written as:

$$IDR - IDR_{max} \leq 0 \quad (7)$$

3 Benchmark case studies

Six benchmark case studies in the optimum structural design of RC frames are considered. Each benchmark is designated by the letter B followed by the benchmark number. The corresponding RC frames are shown in Fig. 3. Furthermore, Tables 1-6 present the design parameters of the optimization problems. For the RC frames, the number of spans ranges between 1 and 3 and the number of storeys between 2 and 6. Equal spans are considered with lengths ranging between 5m and 6m. Storey height is always 3m. Concrete class varies between C20/25 and C30/37 and steel reinforcement class is always B500 following the specifications of EC2. Concrete cover to the centroid of steel reinforcement is always assumed 50mm.

The concrete buildings are designed to withstand dead, live and either wind or earthquake loads. The dead g (kN/m) and live q (kN/m) loads are applied to the beam members in the form of uniformly distributed loads with values specified in Tables 1-6, which are exclusive of beams' self-weight. The wind pressure is applied, for simplicity, in the form of a uniform lateral pressure along the building vertical surfaces and in all possible directions. The seismic action is applied in the form of Eurocode 8 – Type I response spectrum with prescribed design PGA values and soil types (see Tables 3, 5 & 6). Importance class II and behaviour factor $q = 1.5$ are always assumed, herein, following Eurocode 8 recommendations for low ductility class. Furthermore, it is specified that inter-storey drifts for the frequent earthquake should remain below 1%, assuming non-structural elements not interfering with structural deformations. It is noted that DCL is examined herein not because it is the most efficient seismic design approach, but due to the similarities with EC2 design methodologies. A different suite of benchmarks can be developed for the ductile seismic design of RC frames.

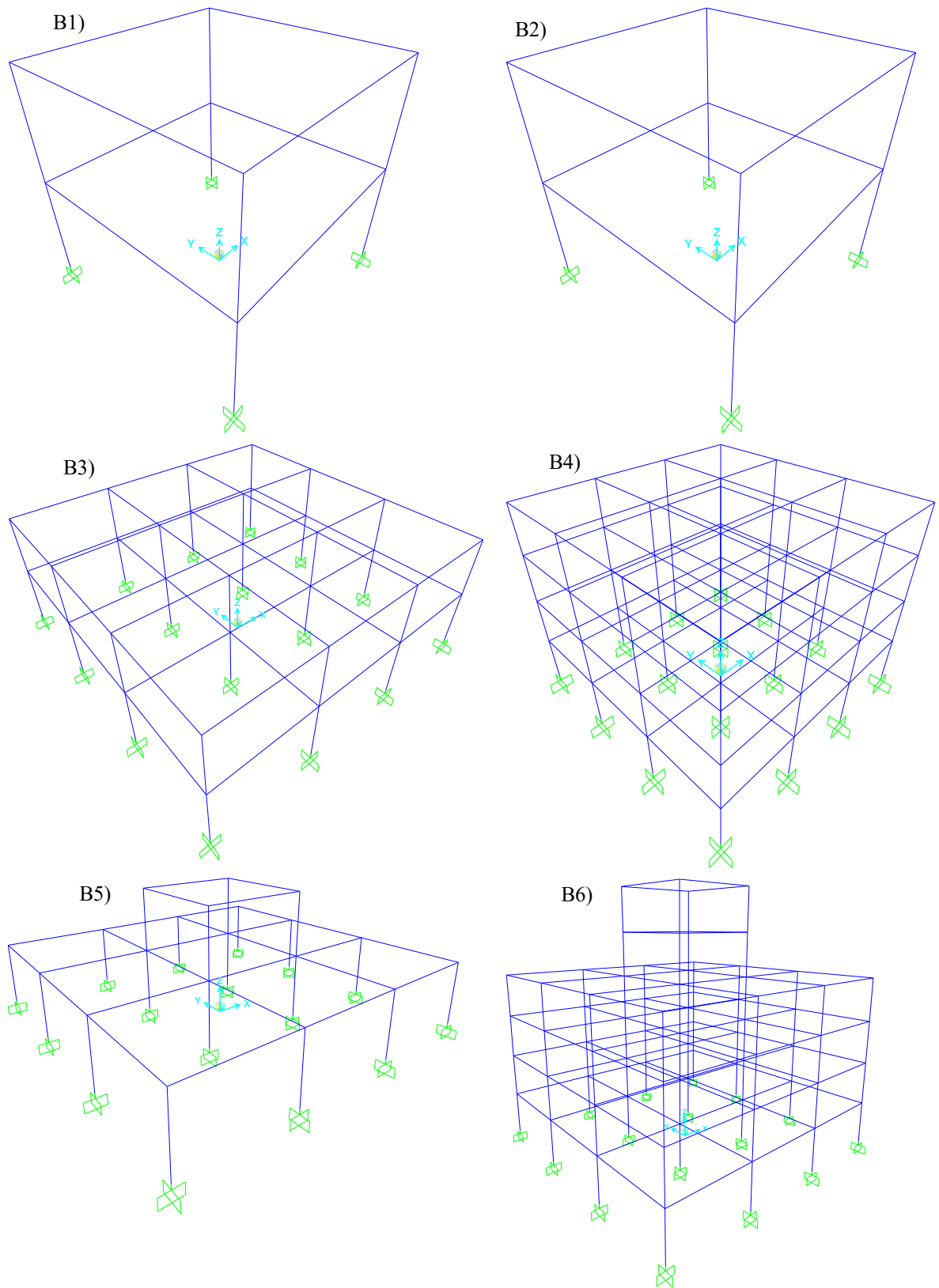


Fig. 3: Benchmark RC frames

Table 1: Design parameters of Benchmark 1

Benchmark 1			
Materials:	C20/25 and B500		
Geometry:	Two-storey, portal frame. Span length of 6m in both directions. Storey height of 3m.		
Loads:	$g = 10.5 \text{ kN/m}$; $q = 7.5 \text{ kN/m}$ applied to all beams. Lateral wind pressure of 2kPa.		
Problem:	$d = 2$; $\Omega = 10^2$; $F_{min} = 1350.8 \text{ €}$		
Group number / Design variable	Description	List of available sections	Optimal Section
1	All beams	0.30X0.30, 0.35X0.30, ..., 0.75X0.30	0.40X0.30
2	All columns	0.30X0.30, 0.40X0.40, ..., 0.75X0.75	0.30X0.30

Table 2: Design parameters of Benchmark 2

Benchmark 2			
Materials:	C20/25 and B500		
Geometry:	Two-storey, portal frame. Span length of 6m in both directions. Storey height of 3m.		
Loads:	$g = 10.5 \text{ kN/m}$; $q = 7.5 \text{ kN/m}$ applied to 1 st storey beams. $g = 25.5 \text{ kN/m}$; $q = 3.0 \text{ kN/m}$ applied to 2 nd storey beams. Lateral wind pressure of 2 kPa.		
Problem:	$d = 3$; $\Omega = 10^3$; $F_{min} = 1476.5 \text{ €}$		
Group number / Design variable	Description	List of available sections	Optimal Section
1	1 st storey beams	0.30X0.30, 0.35X0.30, ..., 0.75X0.30	0.35X0.30
2	2 nd storey beams	0.30X0.30, 0.35X0.30, ..., 0.75X0.30	0.55X0.30
3	All columns	0.30X0.30, 0.40X0.40, ..., 0.75X0.75	0.30X0.30

Table 3: Design parameters of Benchmark 3

Benchmark 3			
Materials:	C25/30 and B500		
Geometry:	Two-storey, three-bay frame. Three spans of 5m in both directions. Storey height of 3m.		
Loads:	$g = 7.5 \text{ kN/m}$; $q = 2.5 \text{ kN/m}$ applied to all exterior beams. $g = 15.0 \text{ kN/m}$; $q = 5.0 \text{ kN/m}$ applied to all interior beams. Seismic action from Eurocode 8 – Type I response spectrum for PGA = 0.36g; Soil type B; Importance Class II; Ductility Class Low; $q = 1.5$		
Problem:	$d = 4$; $\Omega = 10^4$; $F_{min} = 10918 \text{ €}$		
Group number / Design variable	Description	List of available sections	Optimal Section
1	Exterior beams	0.30X0.30, 0.35X0.30, ..., 0.75X0.30	0.30X0.30
2	Interior beams	0.30X0.30, 0.35X0.30, ..., 0.75X0.30	0.35X0.30
3	Exterior (corner and perimeter) columns	0.30X0.30, 0.40X0.40, ..., 0.75X0.75	0.35X0.35
4	Interior columns	0.30X0.30, 0.40X0.40, ..., 0.75X0.75	0.75X0.75

Table 4: Design parameters of Benchmark 4

Benchmark 4	
Materials:	C25/30 and B500
Geometry:	Four-storey, three-bay frame. Three spans of 5m in both directions. Storey height of 3m.
Loads:	$g = 7.5 \text{ kN/m}$; $q = 6.25 \text{ kN/m}$ applied to all exterior beams of first 3 storeys. $g = 15.0 \text{ kN/m}$; $q = 12.5 \text{ kN/m}$ applied to all interior beams of first 3 storeys. $g = 20.0 \text{ kN/m}$; $q = 2.5 \text{ kN/m}$ applied to all exterior beams of the 4 th storey. $g = 40.0 \text{ kN/m}$; $q = 5.0 \text{ kN/m}$ applied to all interior beams of the 4 th storey.

	Lateral wind pressure of 1.5 kPa.		
Problem:	$d = 6$; $\Omega = 7^6$; $F_{min} = 13553$ €		
Group number / Design variable	Description	List of available sections	Optimal Section
1	First three storeys exterior beams	0.30X0.30, 0.35X0.30, ..., 0.60X0.30	0.30X0.30
2	First three storeys interior beams	0.30X0.30, 0.35X0.30, ..., 0.60X0.30	0.40X0.30
3	4 th storey exterior beams	0.30X0.30, 0.35X0.30, ..., 0.60X0.30	0.35X0.30
4	4 th storey interior beams	0.30X0.30, 0.35X0.30, ..., 0.60X0.30	0.50X0.30
5	Exterior (corner and perimeter) columns	0.30X0.30, 0.40X0.40, ..., 0.60X0.60	0.35X0.35
6	Interior columns	0.30X0.30, 0.40X0.40, ..., 0.60X0.60	0.45X0.45

Table 5: Design parameters of Benchmark 5

Benchmark 5			
Materials:	C25/30 and B500		
Geometry:	Two-storey, three-bay frame with setback at the 2 nd storey. All span lengths are 5m. Storey height of 3m.		
Loads:	$g = 7.5$ kN/m; $q = 6.25$ kN/m applied to all exterior beams of first storey. $g = 15.0$ kN/m; $q = 12.5$ kN/m applied to all interior beams of first storey. $g = 7.5$ kN/m; $q = 2.5$ kN/m applied to all 2 nd storey beams. Seismic action from Eurocode 8 – Type I response spectrum for PGA = 0.24g; Soil type A; Importance Class II; Ductility Class Low; $q = 1.5$		
Problem:	$d = 5$; $\Omega = 9^5$; $F_{min} = 4964.3$ €		
Group number / Design variable	Description	List of available sections	Optimal Section
1	First storey exterior beams	0.30X0.30, 0.35X0.30, ..., 0.70X0.30	0.40X0.30
2	First storey interior beams	0.30X0.30, 0.35X0.30, ..., 0.70X0.30	0.50X0.30
3	Second storey beams	0.30X0.30, 0.35X0.30, ..., 0.70X0.30	0.35X0.30
4	All exterior columns	0.30X0.30, 0.35X0.35, ..., 0.70X0.70	0.40X0.40
5	All interior columns	0.30X0.30, 0.35X0.35, ..., 0.70X0.70	0.40X0.40

Table 6: Design parameters of Benchmark 6

Benchmark 6			
Materials:	C30/37 and B500		
Geometry:	Six-storey, three-bay frame with setbacks at the 5 th and 6 th storeys. All span lengths are 6m. Storey height of 3m.		
Loads:	$g = 9.0$ kN/m; $q = 7.5$ kN/m applied to all exterior beams. $g = 18.0$ kN/m; $q = 15.0$ kN/m applied to all interior beams. Seismic action from Eurocode 8 – Type I response spectrum for PGA = 0.16g; Soil type C; Importance Class II; Ductility Class Low; $q = 1.5$		
Problem:	$d = 7$; $\Omega = 6^7$; $F_{min} = 30060$ €		
Group number / Design variable	Description	List of available sections	Optimal Section
1	1 st and 2 nd storey exterior beams	0.30X0.30, 0.40X0.30, ..., 0.80X0.30	0.40X0.30
2	1 st and 2 nd storey interior beams	0.30X0.30, 0.40X0.30, ..., 0.80X0.30	0.50X0.30
3	3 rd and 4 th storey exterior beams	0.30X0.30, 0.40X0.30, ..., 0.80X0.30	0.40X0.30
4	3 rd and 4 th storey interior beams	0.30X0.30, 0.40X0.30, ..., 0.80X0.30	0.50X0.30
5	5 th and 6 th storey beams	0.30X0.30, 0.40X0.30, ..., 0.80X0.30	0.30X0.30
6	Exterior (perimeter & corner) columns	0.30X0.30, 0.40X0.40, ..., 0.80X0.80	0.40X0.40
7	Interior columns	0.30X0.30, 0.40X0.40, ..., 0.80X0.80	0.50X0.50

For non-seismic actions, design action effects are calculated by 3D linear elastic static analysis with the aid of SAP2000. Beam and column members are modelled by 3D elastic frame elements with uncracked (i.e. geometric) structural properties. No moment redistribution is considered. For column members, the design bending moments are increased to account for geometric imperfections and 2nd order effects. For seismic actions, actions effects are determined by linear elastic response-spectrum analysis. Cracked stiffness for the concrete members is used in that is assumed to be 50% of the uncracked, following the recommendations of EC8 [42]. Floor masses are assumed to be lumped at the floor centres. Furthermore, diaphragmatic action is considered in the plane of each floor. In all cases, fixed supports are assumed at the column bases.

The RC frames are divided into beam and column member groups with the same cross-section. The numbering, description and list of available cross-sections for each group of structural members are presented in Tables 1-6. It is recalled that all available cross-sections follow the general configurations of Fig. 2 for beam and column members. Different configurations may drive to different optimal solutions. It is also reminded that the numbering and total number of groups of the RC frames coincides with the numbering and total number of independent design variables d (i.e. dimensions), respectively, in the optimization problem. The dimensions of the benchmark case studies range between $d = 2$ and $d = 7$. Moreover, the search spaces Ω range between $\Omega = 10^2$ and $\Omega = 6^7 (= 279,936)$ discrete candidate design solutions.

4 Exhaustive search

In this section, the results of exhaustive search analysis of the six benchmark RC frames are presented. It is noted that all results are included in the accompanying file of this manuscript, Benchmarks.xlsx, so that they can be used by readers in future optimization studies. Exhaustive search examines all candidate design solutions (i.e. all combinations of groups' cross-sections)

whether they satisfy constraints and then calculates their objective function values. The main advantage of exhaustive search is that it guarantees tracking of global optimum solutions in a prescribed discrete search space of available cross-sections. The latter is the case independently of the geometry of cross-sections and types of constraints. Furthermore, it can offer valuable insights into the landscape of objective functions. On the negative side, it is accompanied by high computational costs that make it prohibitive for large-scale optimization problems.

The exhaustive search results are presented in Figs 4 to 8 in terms of concrete volume V_c , mass of steel reinforcement m_s , inclusive of both longitudinal bars and shear links, and economic cost of the RC frames as a whole. The economic cost is calculated herein by Eq. (2) assuming a typical unit price of concrete $f_{co} = 100 \text{ €/m}^3$ and a typical unit price of steel reinforcement $f_{so} = 1 \text{ €/kg}$. Only feasible solutions are presented in the figures that satisfy all design constraints. Furthermore, the obtained global optimum solutions of the benchmark case studies are shown in Tables 1-6 together with their corresponding economic costs F_{min} .

Figure 4 presents the variation of total cost with the concrete volume of the RC frames. It is shown that, for all benchmark case studies, as the concrete volume increases the total cost first decreases and then increases. Therefore, the optimal solutions are always between the solutions for minimum and maximum concrete volumes. This contradicts a common misconception in structural design of RC frames that minimum concrete volume designs are also the most cost-efficient structural solutions. This is not the case, however, since too small concrete sections can increase sharply the requirement for steel reinforcement increasing thereby the total economic cost.

Moreover, Fig. 5 illustrates the variation of RC frames total cost versus the mass of steel reinforcement. Similarly to V_c , the cost of RC frames first decreases and then increases as the mass of steel increases. It is, therefore, concluded that the optimum cost solution does not coincide with the solutions for minimum and maximum steel reinforcement mass. Instead, it

represents the best compromise between the requirements for concrete and steel reinforcement quantities.

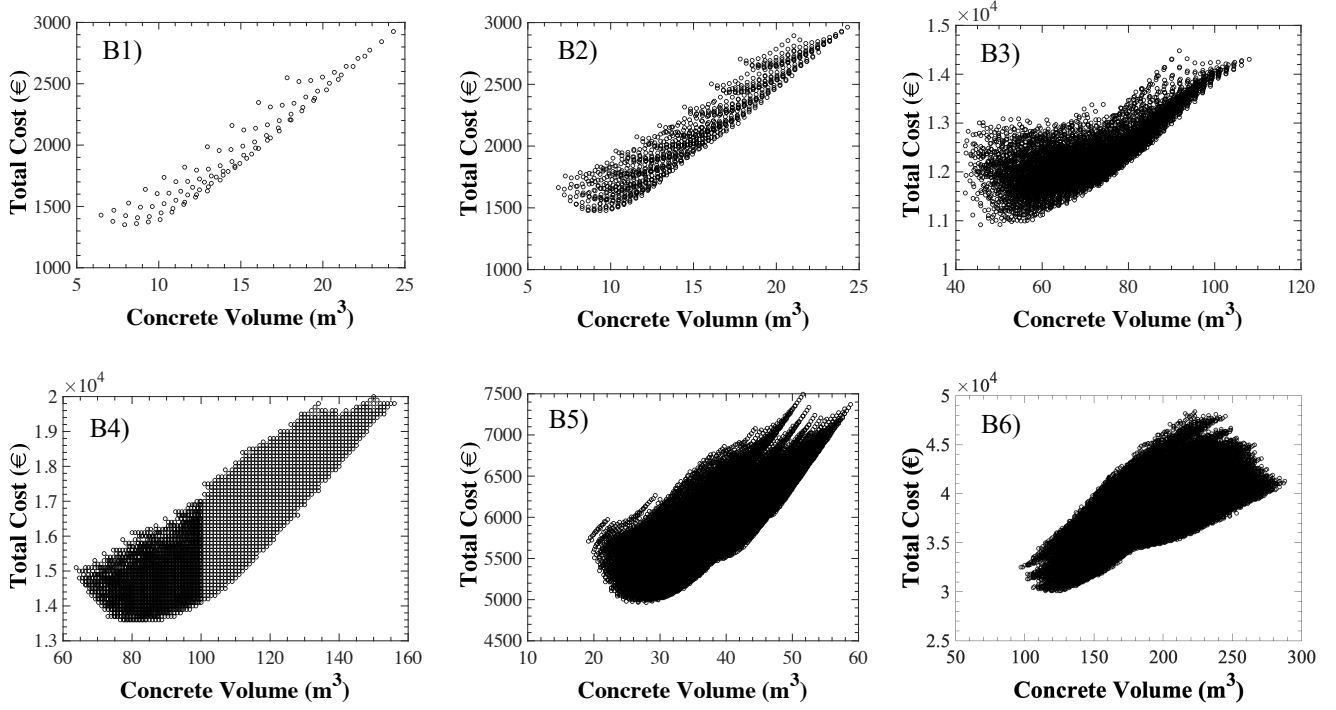


Fig. 4: Total cost versus concrete volume

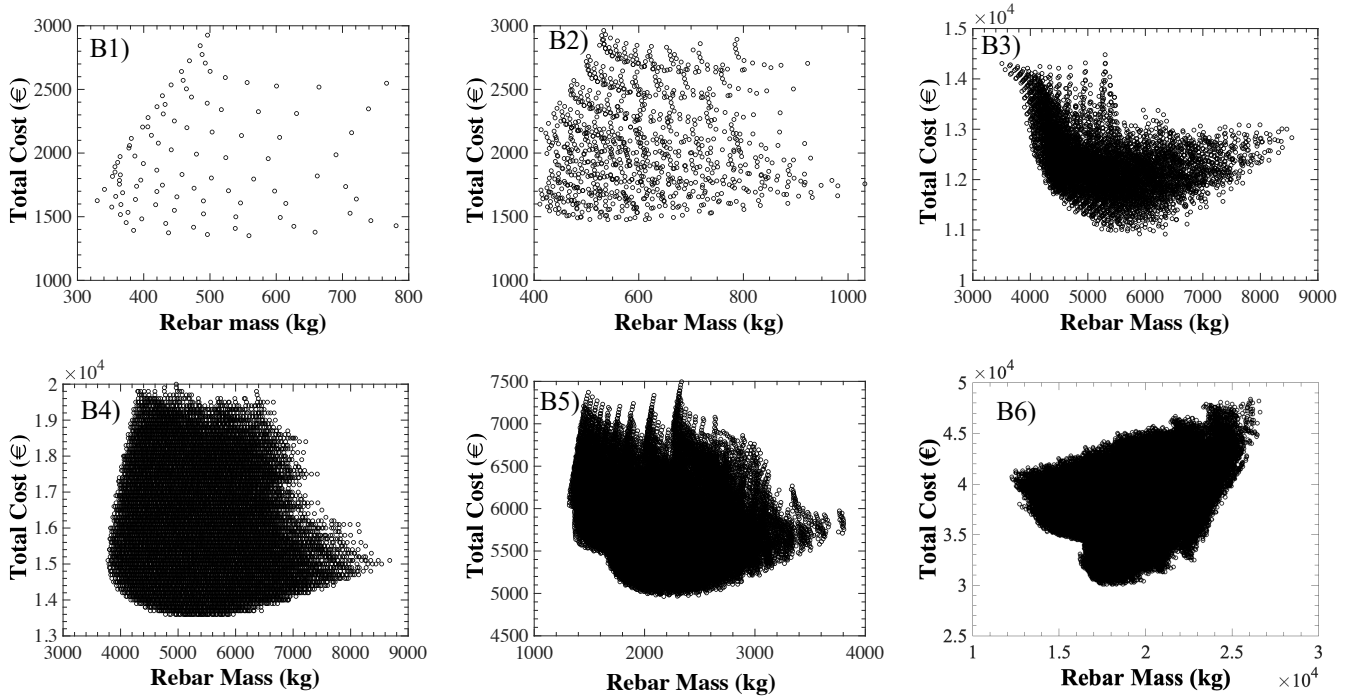


Fig. 5: Total cost versus steel reinforcement mass

Figure 6 shows the variation of total cost with the ratio of steel reinforcement mass to concrete volume (m_s/V_c). The latter ratio quantifies the relative amount of steel reinforcement in concrete. It is often believed that efficient design solutions of RC frames have m_s/V_c ratios within a small range of values. Consequently, this ratio is widely used as an indicator of optimum design solutions. Nevertheless, Fig. 6 illustrates that optimal m_s/V_c ratios vary significantly across the various benchmark case studies and therefore are rather problem specific. Figure 6 reveals also that, for the same case study, a wide range of m_s/V_c ratios may yield costs very similar to the optimal solution. Therefore, the optimal costs are not particularly sensitive to m_s/V_c ratios. Finally, it is worth mentioning that, for the same case study, design solutions with similar m_s/V_c ratios may have completely different total costs.

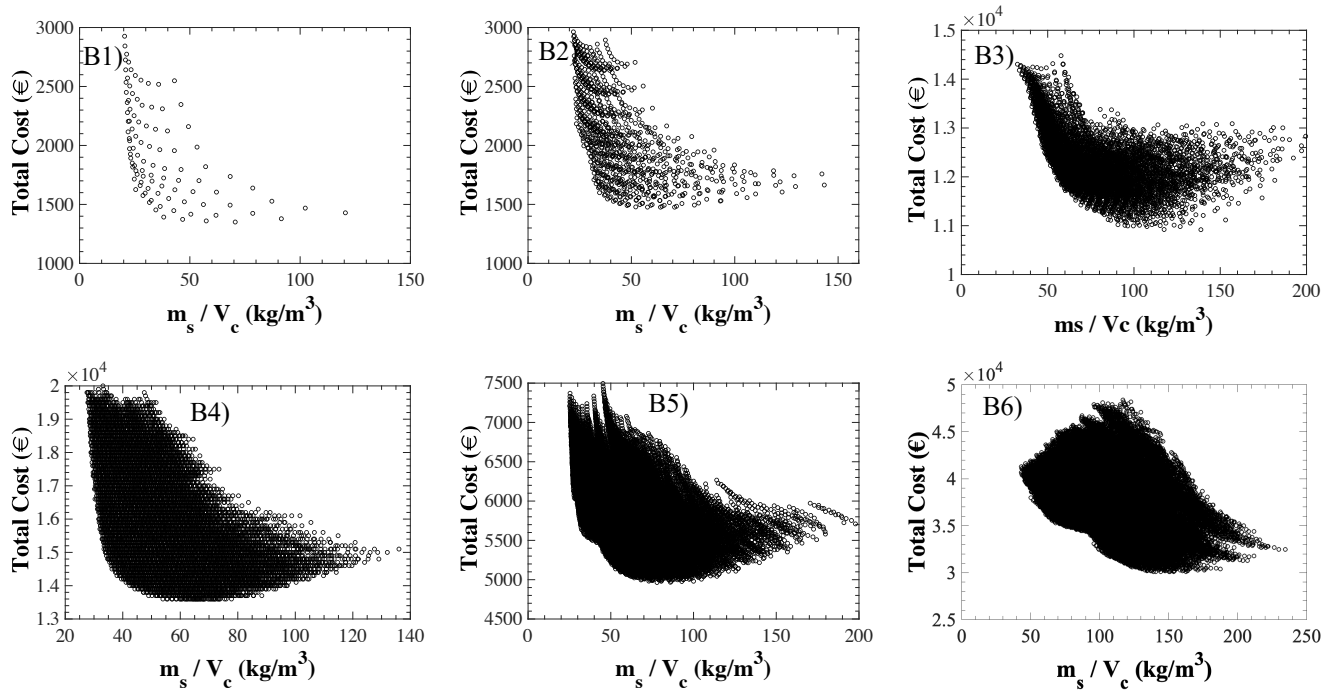


Fig. 6: Total cost versus steel reinforcement mass to concrete volume ratio

Figure 7 presents the relationship between the required steel reinforcement mass and the concrete volume of RC frames. Generally, it is observed that as the concrete volume increases the requirement of steel reinforcement decreases. Therefore, decreasing concrete volume and reducing steel mass are conflicting objectives with well-formed Pareto fronts. However, it is interesting to note that, for large concrete volumes, m_s tends to increase with V_c . This is explained by the fact that the calculation of steel reinforcement in these cases is dominated by the provisions for minimum steel reinforcement as percentage of cross-sectional areas.

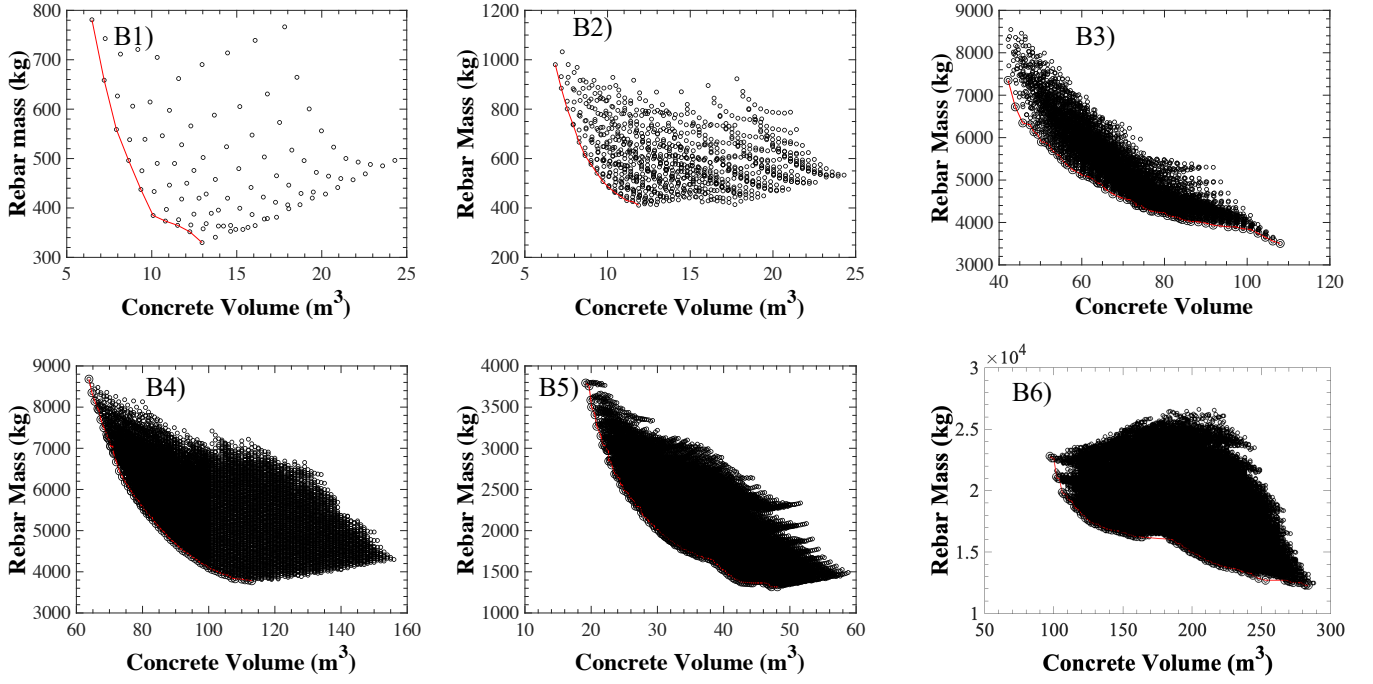


Fig. 7: Steel reinforcement mass versus concrete volume

Figure 8 shows the relationship between m_s/V_c ratios and the concrete volume of RC frames. As expected, a more competitive relationship between m_s/V_c and V_c is observed, than the m_s versus V_c relationship, since the steel mass is now divided by the concrete volume. It is also noted that, for large V_c values, m_s/V_c ratios seems to remain practically unchanged with increasing V_c since the designs are controlled by minimum reinforcement provisions.

Figure 9 attempts to give a further insight into the landscapes of B1-B3 objective functions. For B1, it is observed that the cost monotonically decreases as the optimal solution with column section height of 0.30m and beam section height of 0.40m is approached. For B2, the variation of total cost versus the section heights of 1st and 2nd storey beams is presented for the optimal column section of 0.30mX0.30m. Again, it is seen that the total cost monotonically reduces as the optimal solution with bottom beams of 0.30X0.35 and top beams of 0.30X0.55 is reached. For B3, the variation of total cost with the heights of interior beams and exterior columns is presented. In this figure, the exterior beams and interior columns are assumed to have fixed sections that correspond to the global optimum solution for this problem (i.e.

0.30X0.30m for exterior beams and 0.75X0.75m for interior columns as shown in Table 3). It is seen now that two local optimum solutions are revealed. Both solutions have exterior column section heights of 0.35m. However, the first solution has interior beam section height of 0.35m and the second solution a respective height of 0.55m. The former beam section height corresponds to the global optimum solution (see Table 3). This observation is important as it shows that objective functions of these optimization problems may be multimodal and therefore global optimization algorithms and procedures are required to track global optima.

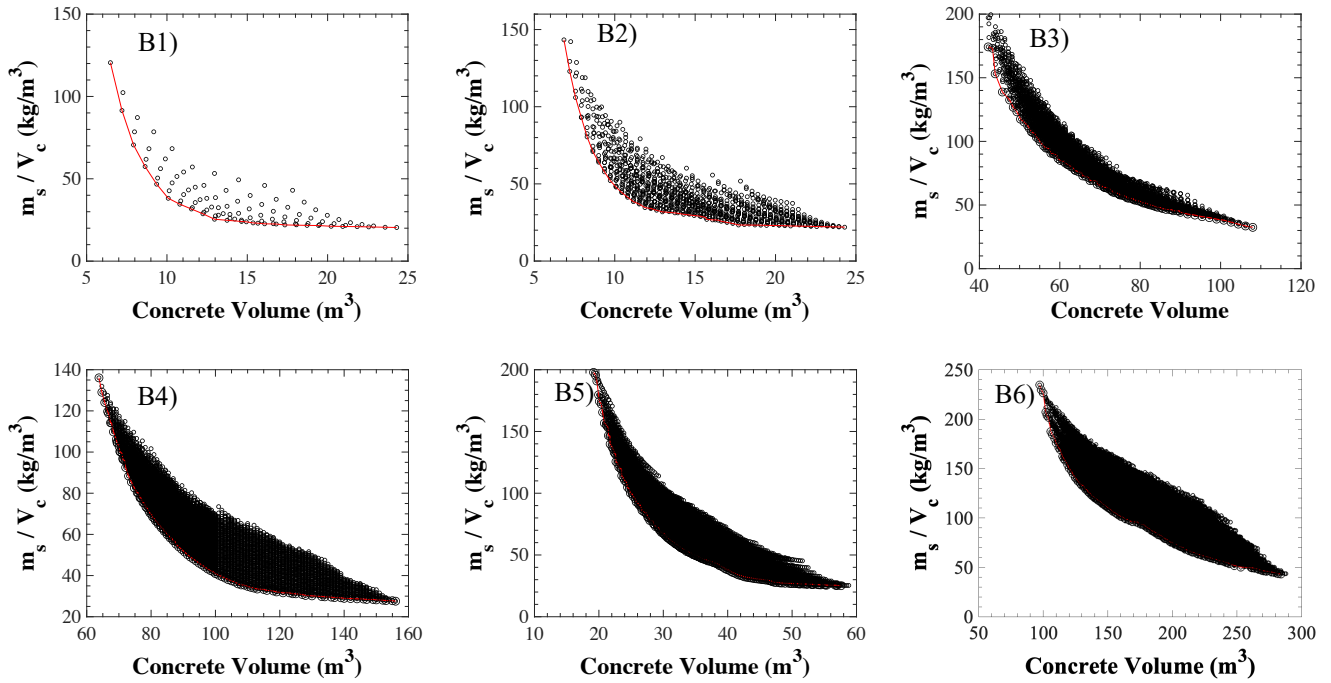


Fig. 8: Steel reinforcement mass to concrete volume ratio (m_s/V_c) versus concrete volume

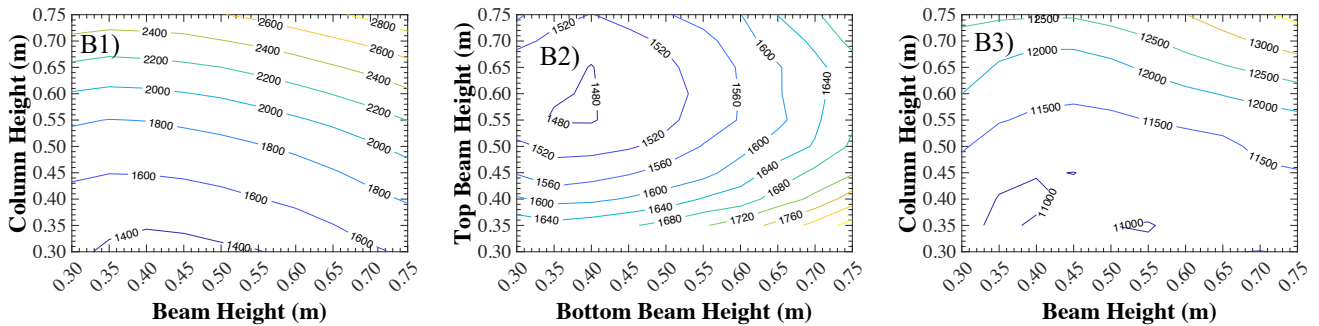


Fig. 9: Contour plots of total costs versus cross-sectional dimensions

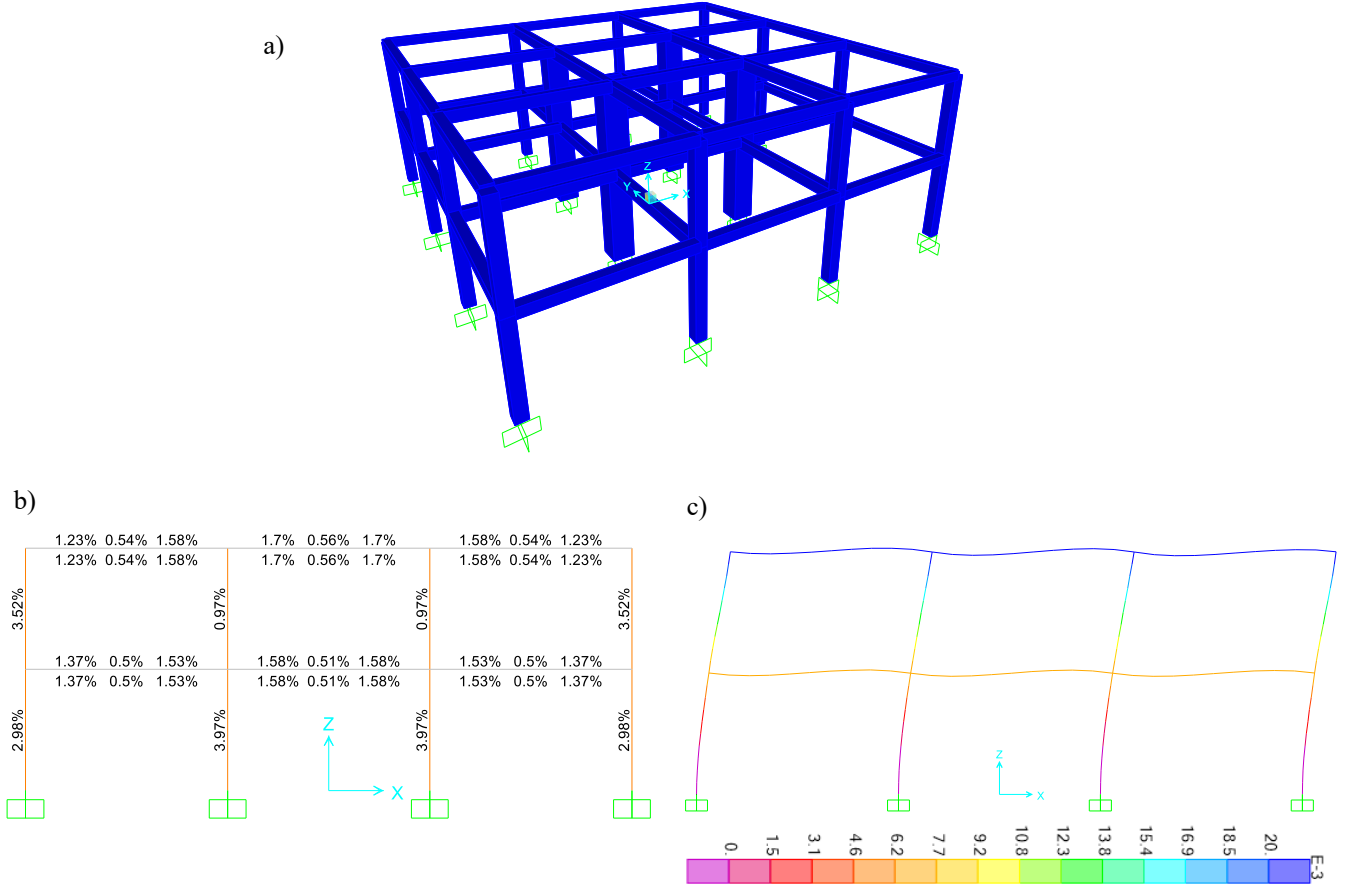


Fig. 10: Optimal design solution of benchmark B3; a) 3D geometry; b) $\rho_l(\%)$ ratios; c) deflections under the frequent earthquake of an interior plane frame

At this stage, it is worthy to shed more light into the optimal design solution of B3 as an indicative example of the ability of the proposed approach to track valid global optimum solutions. Figure 10a presents the 3D geometry of the optimal B3 design solution with cross-sections shown in Table 3. It is interesting to see that the algorithm has selected the largest cross-sections for the four interior columns and small cross-sections for all other members. This concentrates seismic actions in a small number of structural members and relieves other members. Furthermore, Fig. 10b shows the ρ_l ratios of all members of an interior plane frame of the 3D structure. It is noted that the ρ_l ratios of the ground-storey interior columns are 3.97%, which is slightly below the limit of 4% set by EC2 [41]. Furthermore, Fig. 10c presents the deformed configuration of the same frame under the frequent earthquake design action. It is shown that the top displacement remains below 0.02m meaning that inter-storey drifts remain well below 1% that is set as design constraint.

5 Single-objective optimization algorithms

In this section, the performance of various well-established single objective optimization algorithms against the benchmark case studies is examined. The objective function examined in this section is the total economic cost of the RC frames as specified in §4. The goal, herein, is to make conclusions regarding the ability of common single objective algorithms to track global optimum solutions of small-scale problems in structural design of RC frames and the required computational cost to achieve so.

More particularly, six optimization algorithms are investigated, namely, the Pattern Search (PS) [48], Genetic Algorithm (GA) [49], Flower Pollination Algorithm (FPA) [50], Particle Swarm Optimization (PSO) [51], Simulated Annealing [52] and Surrogate Based Optimization (SBO) [48] framework. PS investigates a set of points around the current design solution and updates the latter iteratively when a better solution is identified. GA is a population-based metaheuristic optimization algorithm inspired by Darwin's theory of evolution. FPA is another nature-inspired, population-based optimization algorithm reproducing the pollination process of flower species. PSO is again a metaheuristic, population-based algorithm imitating the motion of bird flocks and fish schools. SA evolves a candidate design solution based on the annealing process in metallurgy. SBO frameworks employ surrogates to predict the values of computationally expensive objective functions, such as the objective function of the present study due to the numerous and computationally costly finite element analyses and structural design calculations required [28]. It is clarified that all algorithms applied in this section, apart from FPA, are formulated as described in MathWorks [48] and used as implemented in MathWorks [45].

For each algorithm and benchmark case study, 10 independent runs are conducted to account for the stochastic nature of the optimization algorithms. All runs are terminated when either

the global optimum solution is tracked or when a maximum number of function evaluations is reached. The latter is assumed to be equal to the number of exhaustive search design solutions, as shown in Tables 1-6. For all population-based algorithms, a population size of 10 is assumed for benchmarks B1 and B2 and of 20 individuals for problems B3 to B6. All remaining parameter options of the optimization algorithms are set according to the recommendations in MathWorks [48]. For the FPA algorithm, the parameter settings suggested in Mergos and Yang [35] are assumed.

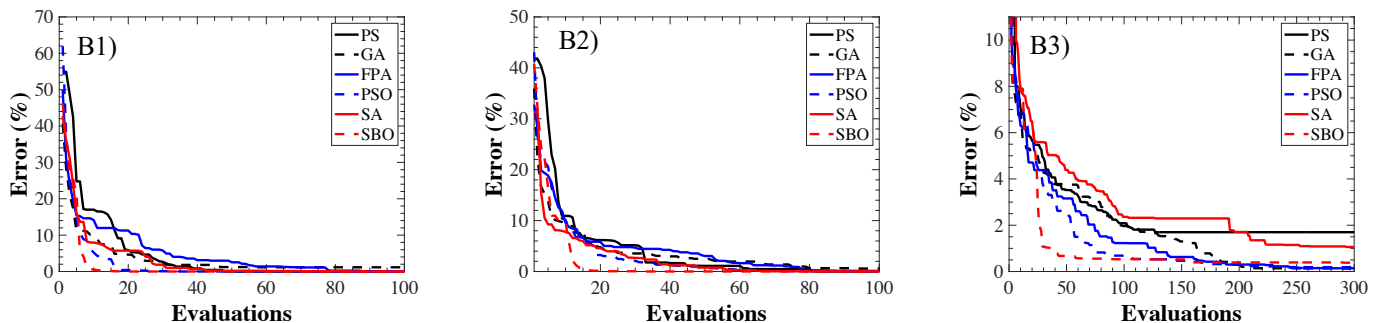
It is worth noting herein that the performance of the various optimization algorithms strongly depends on their parameter settings. Therefore, the conclusions made in the following are specific to the applied algorithmic instances (i.e. algorithms + parameter settings) rather than the algorithms themselves. A parameter tuning study (e.g. [35]) aiming at maximising the performance of these algorithms for the benchmark case studies under investigation is out of the scope of the present study. The aim here is simply to demonstrate and investigate the performance of common optimization algorithms with typical parameter settings.

Figure 11 presents the average optimization histories, of the 10 independent runs, for the different optimization algorithms and benchmark case studies. These histories are shown in the form of relative cost errors (%) with respect to the global optimum cost, as established by exhaustive search, versus the number of function evaluations. It is shown that all algorithms perform satisfactorily and manage to reduce average errors to less than 2% of global optimum cost within rather limited computational budgets. As expected, the required number of function evaluations to reach a target relative error increases as the number of problem dimensions d (i.e. number of design variables) increases. However, for almost all benchmark case studies and optimization algorithms, $50 \cdot d$ function evaluations seem sufficient to reduce average errors to 2% of the global optimum cost.

It is also observed that the optimization algorithms converge differently, for each benchmark case study, when compared to the other algorithms. For example, the PS demonstrates the

highest convergence speed for benchmarks B4 to B6, but it is slower than other algorithms for B1 to B3. On the other hand, SBO is the speediest algorithm for benchmarks B1-B3, but it is outperformed by other algorithms for B4 to B6. Nevertheless, some general conclusions can be made with respect to the relative convergence performance of the various algorithms. It is concluded that the PS and SBO algorithms converge rather quickly for all benchmark case studies. The GA and PSO algorithms demonstrate, typically, an average convergence performance with respect to the other algorithms. The FPA algorithm seems to be slightly slower than the former algorithms. The SA algorithm is the slowest, on average, of all examined optimization algorithms as it demonstrates the smallest or second smallest convergence rate across the six benchmark case studies.

Figure 12 presents, in the form of box plots, the numbers of function evaluations at which convergence to the global optimum solution (i.e. success) was achieved by the independent runs of the different algorithms. The box plots show the minimum, maximum and median (red line) function evaluations. Inside the boxes, the 25th to 75th percentiles are contained. Only successful algorithm runs are presented in this figure. A run is considered as successful when the global optimal solution is tracked within equal or less function evaluations than exhaustive search. In the opposite case, the use of optimization algorithms seems pointless.



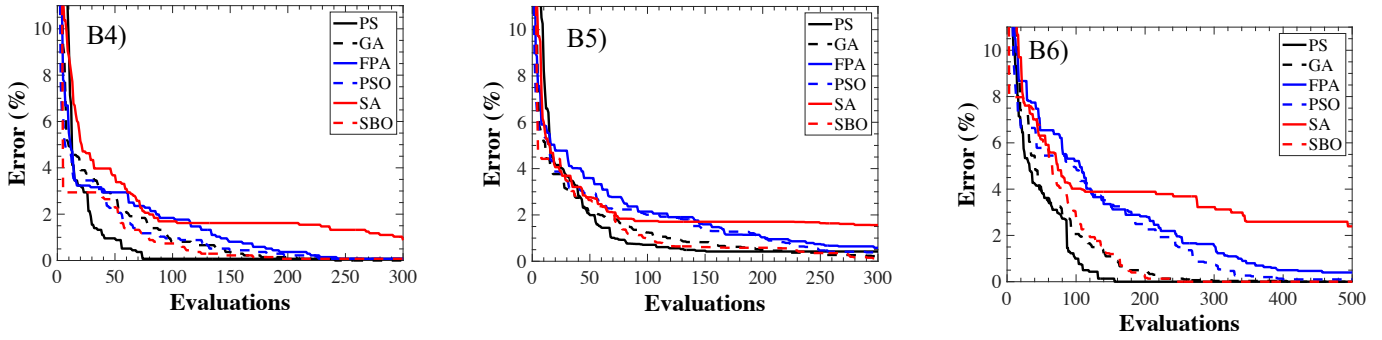


Fig. 11: Single-objective algorithms average optimization histories

The number of successful runs of all optimization algorithms and for all benchmark case studies is also shown in Fig. 13. The fact that all algorithms, apart from SBO, fail several times to get the global optimum solutions within the computational budget of exhaustive search is by itself a matter of concern.

Generally, the PS algorithm seems to be tracking relatively quickly the global optimum solutions for most of benchmark case studies. This is expected as it is a local optimization algorithm with high exploitation capability. However, it also demonstrates the smallest number of successful runs across all benchmark case studies. This is the case because it is susceptible to getting trapped in local optima. The SBO algorithm performs well for all benchmark case studies demonstrating 100% success rate and requiring, typically, small numbers of function evaluations to identify the global optima. It is noted, however, that this algorithm has been found to getting stuck in local optima in larger-scale design problems of concrete frames [28]. The GA and PSO seem to yield average performances, among the various algorithms, in terms of both speed at reaching the global optimal and success rates. The SA is, typically, the slowest algorithm at tracking the global optimum solutions, but its success rates are similar to the PSO and GA algorithms. Finally, the FPA algorithm is generally the second slowest in terms of reaching global optima, but it demonstrates the second-best success rates due to its high exploration abilities [27,50].

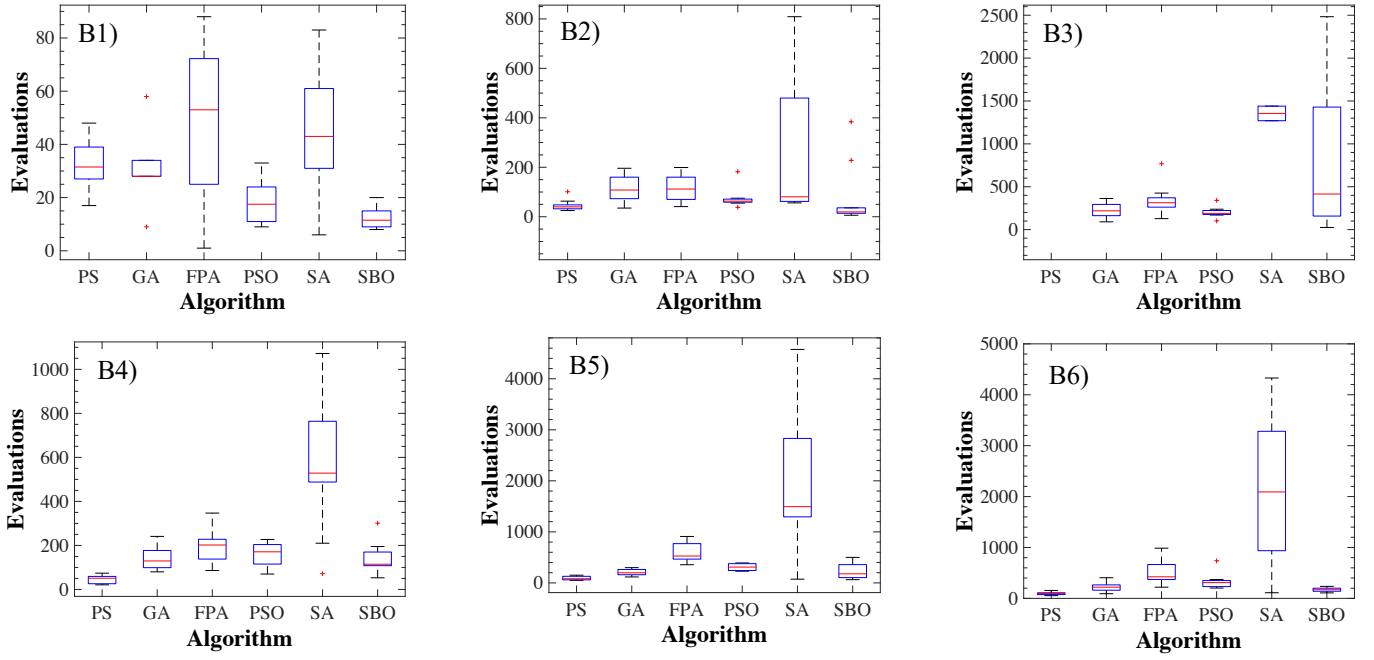


Fig. 12: Number of function evaluations till success

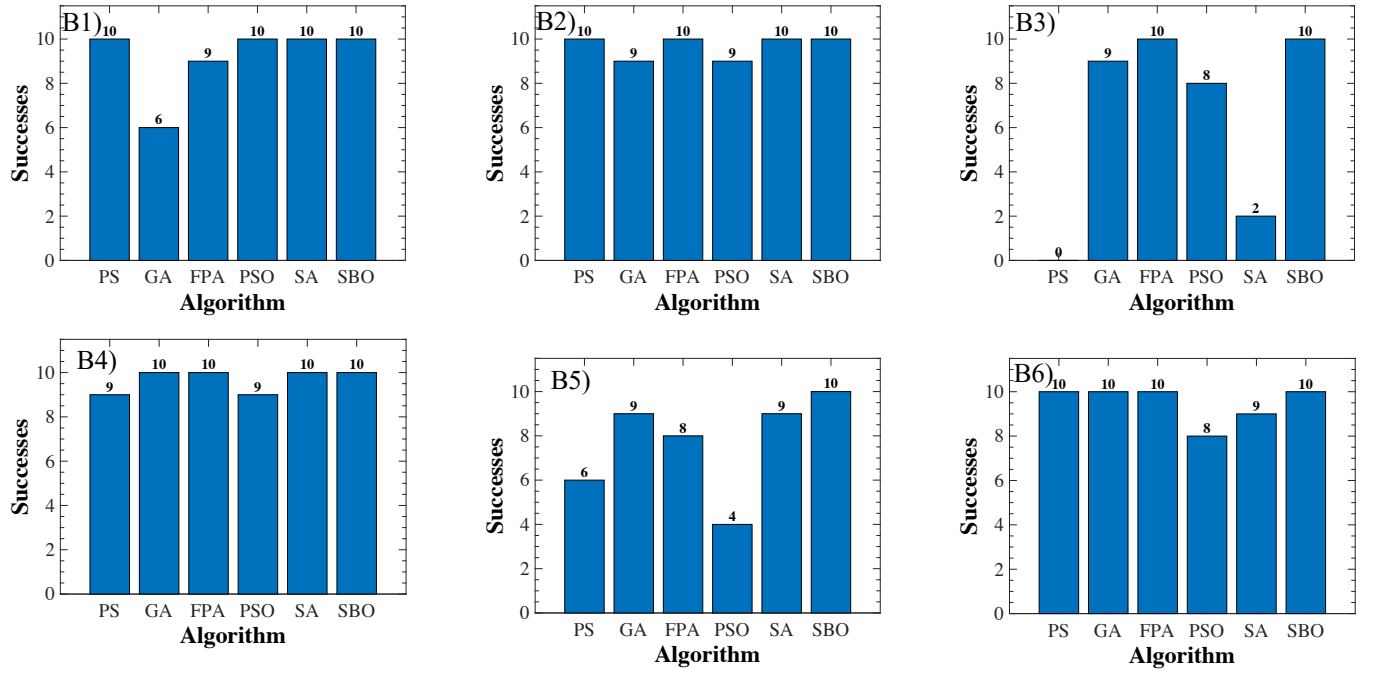


Fig. 13: Number of successful runs

6 Multi-objective optimization algorithms

Herein, the performance of multi-objective optimization algorithms against the benchmark case studies is examined. The two objective functions considered are the mass of steel

reinforcement m_s and the volume of concrete V_c . As discussed in §4, m_s and V_c are highly competitive objectives leading to well-formed Pareto fronts. The goal of this section is to investigate the capability of multi-objective optimization algorithms to predict these Pareto fronts for a given computational budget. Two multi-objective optimization algorithms are examined as implemented in MathWorks [48]. The first algorithm, namely *gamultobj* in MathWorks [48], is an elitist genetic algorithm (GA) that can be considered as a variant of NSGA-II [53]. The second algorithm, namely *paretosearch* in MathWorks [48], employs pattern search (PS) to explore iteratively for non-dominated design solutions.

For each algorithm and benchmark case study, independent runs are conducted with fixed numbers of maximum function evaluations ranging between $50 \cdot d$ and $400 \cdot d$, but smaller than the corresponding exhaustive search design combinations. The calculated Pareto fronts are then compared with the “real” Pareto fronts obtained by exhaustive search. For the GA algorithm, a population size of 10 is assumed for benchmarks B1 and B2 and of 20 individuals for problems B3 to B6 based on the results of a preliminary analysis. All remaining parameter options of the optimization algorithms are set according to the recommendations in MathWorks [48].

The comparisons of the calculated versus the “real” Pareto fronts of all benchmark case studies and algorithm runs are presented in Figs. 14-19. In these figures, each algorithm run is denoted by the abbreviation of the algorithm (i.e. GA or PS) and the applied maximum number of function evaluations (e.g. $50 \cdot d$) that was used as a stopping criterion. It is observed that the PS algorithm performs significantly better than the GA algorithm in all benchmark case studies. Despite the fact that the latter algorithm predicts several non-dominated solutions, it is not able to capture well the full extent of Pareto fronts, even after $400 \cdot d$ trial solutions. Since the NSGA-II is a well-established algorithm, the problem in these analyses is believed to be related to the algorithm parameter options applied rather than the algorithm itself. Tuning of these

parameters to maximize the performance of the algorithm in such optimization problems is a topic worth investigating in future studies.

On the other hand, the PS algorithm seems to yield satisfactory representations of the Pareto fronts that systematically improve as the number of examined design solutions increases. In all cases, very good predictions of the Pareto fronts are obtained between $200 \cdot d$ and $400 \cdot d$ trial solutions. It is noted, however, that not all non-dominated design solutions are identified even after $400 \cdot d$ trial solutions. It is also worth mentioning that, as expected, the multi-objective PS algorithm requires many more trials to converge than the single-objective PS algorithm presented in §5.

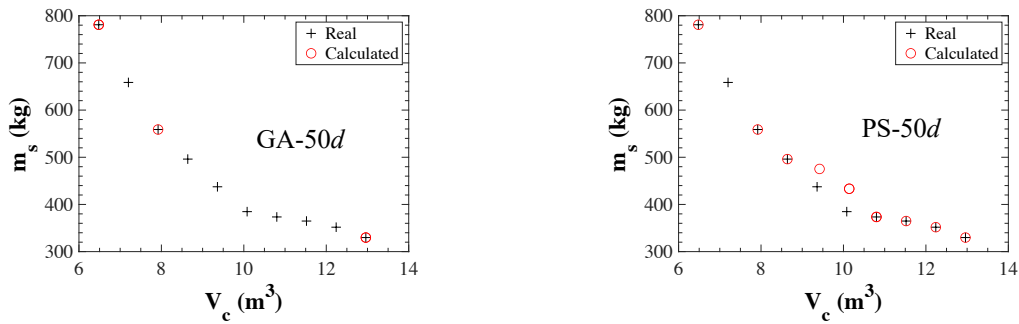


Fig. 14: Steel reinforcement mass versus concrete volume Pareto fronts – Benchmark 1

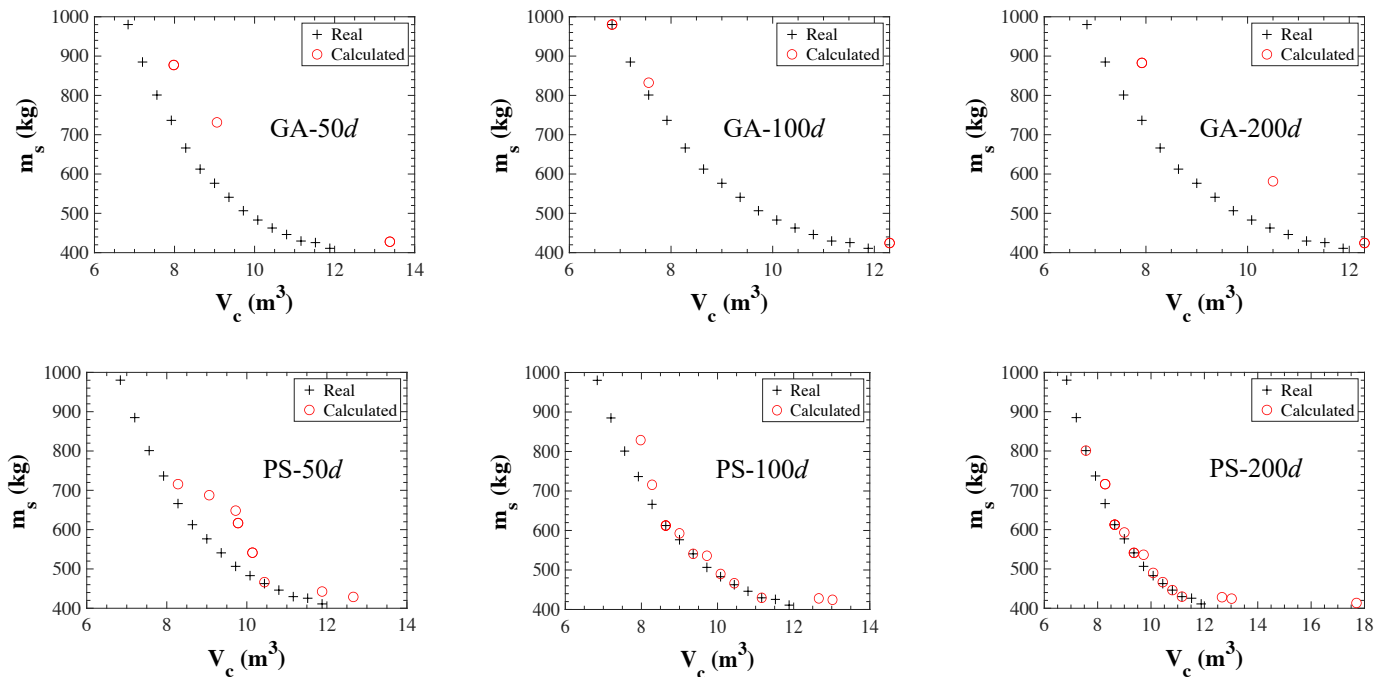


Fig. 15: Steel reinforcement mass versus concrete volume Pareto fronts – Benchmark 2

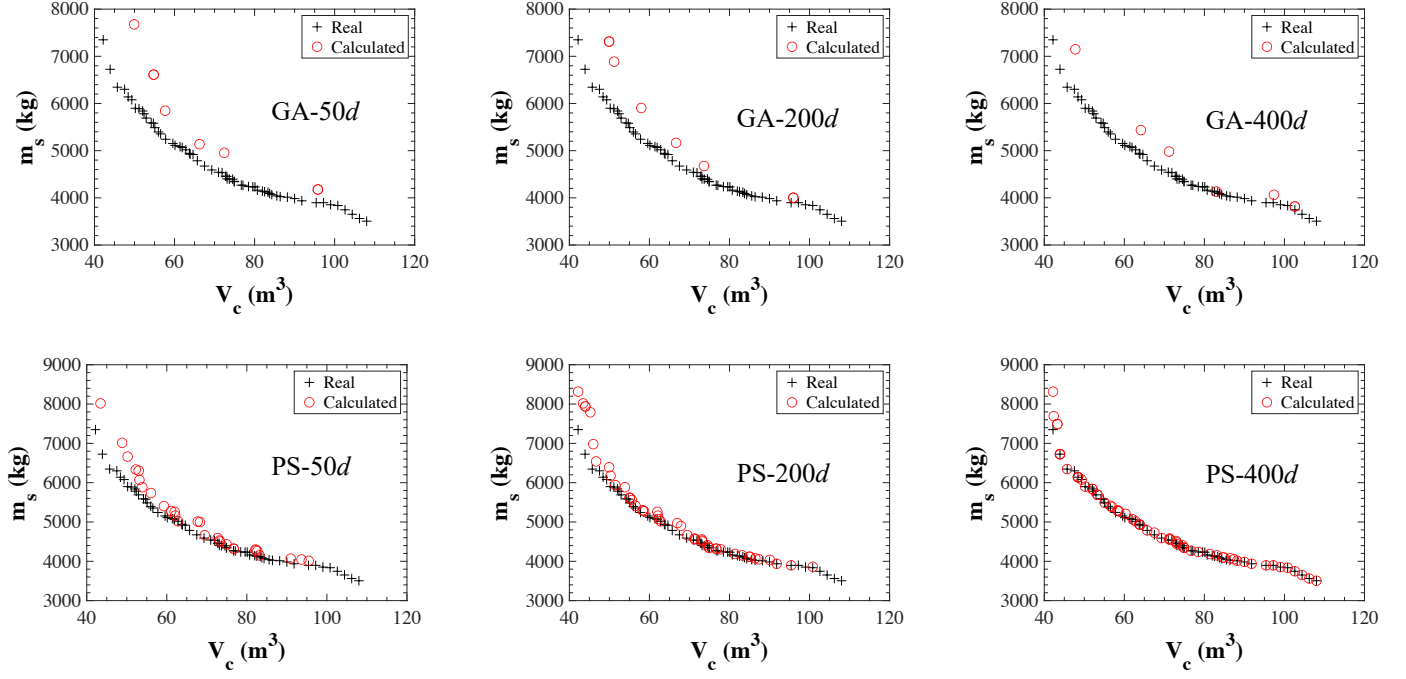


Fig. 16: Steel reinforcement mass versus concrete volume Pareto fronts – Benchmark 3

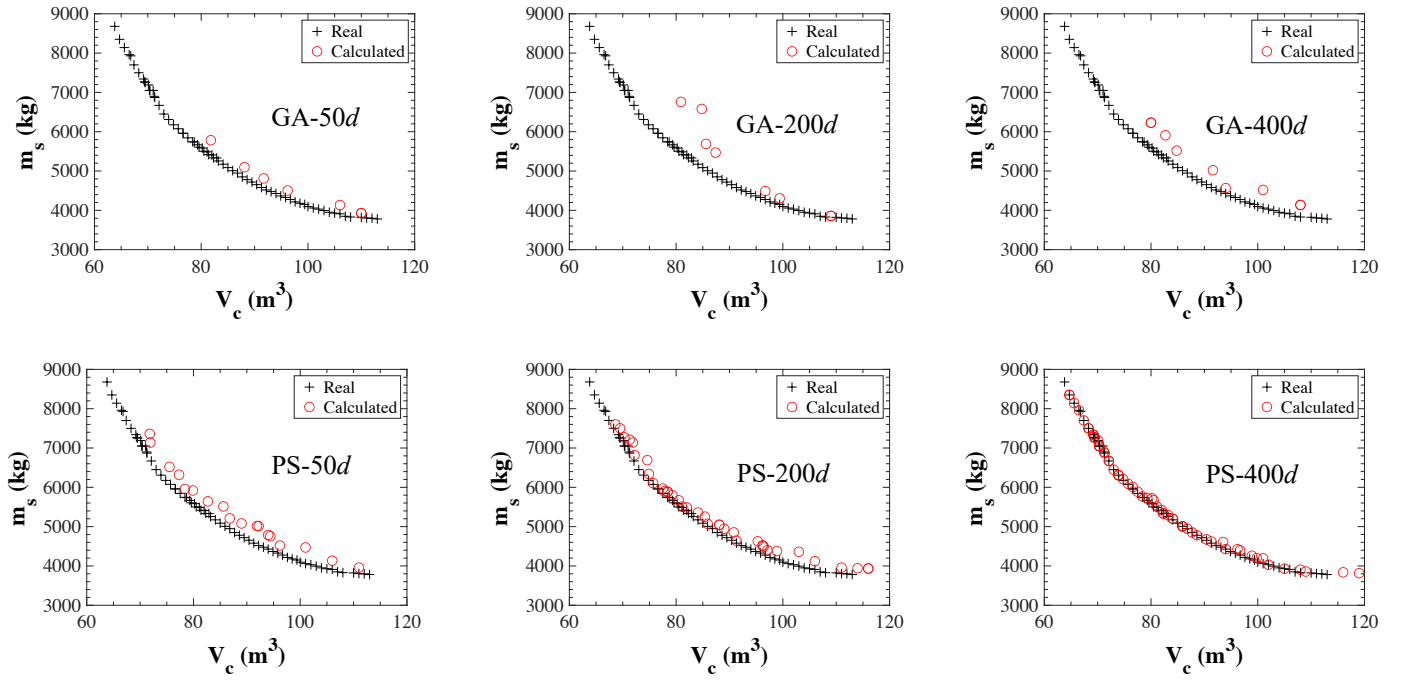


Fig. 17: Steel reinforcement mass versus concrete volume Pareto fronts – Benchmark 4

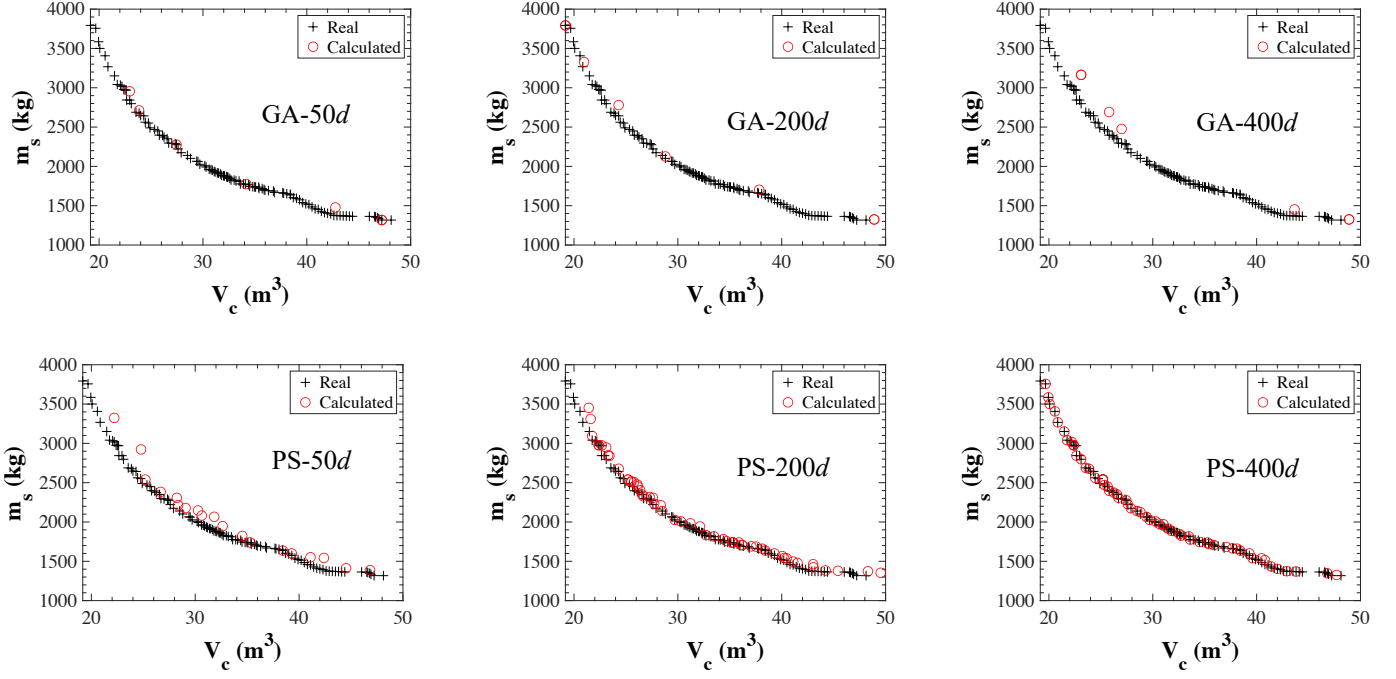


Fig. 18: Steel reinforcement mass versus concrete volume Pareto fronts – Benchmark 5

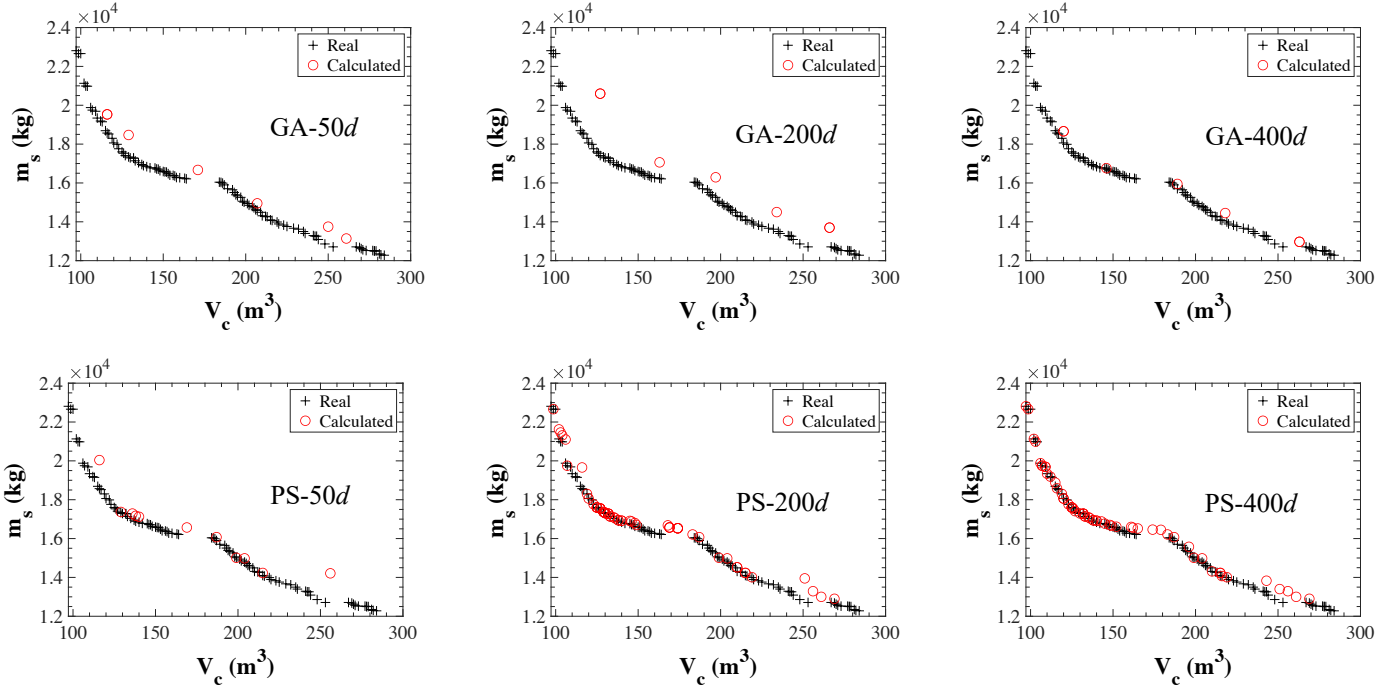


Fig. 19: Steel reinforcement mass versus concrete volume Pareto fronts – Benchmark 6

7 Conclusions

Benchmarking goes hand in hand with the development of efficient optimization methodologies in various scientific fields as it allows for an objective quantification of their

computational performance. Benchmark case studies must be representative of the class of problems being investigated since the performance of optimization techniques cannot be generalised to all problem classes. In the past, several studies have applied optimization methodologies/algorithms to the structural design of concrete frames. Nevertheless, benchmark optimization problems in this area seem to be missing in literature hindering the efficient and reliable optimization of concrete frames.

The present study aims at filling part of this gap in literature by providing small-scale benchmark case studies in the optimum design of 3D concrete frames. The main goal here is that these benchmarks are employed in the future calibration, tuning, improvement and development of direct search methods and evolutionary optimization algorithms to address this class of optimization problems. More particularly, six 3D building RC frames are designed in accordance with Eurocode 2 [41] and Eurocode 8 [42]. The independent design variables of these frames, representing discrete concrete cross-sections of member groups, range between 2 and 7 and the candidate design solutions between 100 and 279,936.

First, exhaustive search analysis of the benchmark case studies is conducted revealing their global optimum solutions and Pareto fronts. In addition, by visualising the results of exhaustive search, useful conclusions are made regarding the relationships between total material cost, concrete volume, and steel reinforcement mass. Useful insights into the landscapes of the objective functions are also provided. All exhaustive search results are provided in an accompanying file of this manuscript so that they can be used in future optimization studies.

Next, six well-established single objective optimization algorithms are applied to minimize the material cost of the benchmark frames, including evolutionary, direct search and surrogate-based algorithms. The performance of these algorithms is quantified in terms of actual errors with respect to the global optimum solutions from exhaustive search. Useful conclusions are made with respect to the overall performance, in terms of speed of convergence and robustness,

of the single objective algorithms in the optimum design of concrete frames as well as the computational cost required to achieve satisfactory results.

Moreover, two multi-objective optimization algorithms are employed to track the steel reinforcement mass versus concrete volume Pareto fronts of the benchmark RC frames. The predicted Pareto fronts for various computational budgets are compared with the actual ones from exhaustive search. It is generally concluded that multi-objective problems are more challenging than single-objective ones and further research is required to establish efficient optimization methodologies tracking satisfactorily actual Pareto fronts with limited computational costs.

Closing this work, the need for further benchmark studies in the optimum design of reinforced concrete structures is emphasized. These studies can focus on larger-scale problems in the optimum design of 2D and 3D concrete frames as well as different types of concrete structures, design methodologies and objective functions such as structural performance and life-cycle cost. This step is considered essential to support and promote the reliable optimization of concrete structures to facilitate sustainable and resilient construction.

Conflict of Interest Statement

On behalf of all authors, the corresponding author states that there is no conflict of interest.

Acknowledgments and Funding Information

No funding was received to assist with the preparation of this manuscript.

Replication of Results

All exhaustive search results of the present study are included in the accompanying file Benchmarks.xlsx so that they can be used in future studies. The results of the optimization algorithms cannot be fully reproduced due to the stochastic nature of these algorithms.

References

1. IEA (2020) Energy technology perspectives 2020. International Energy Agency
2. IPCC (2021) Climate change 2021: The physical science basis. Intergovernmental Panel on Climate Change, Cambridge University Press, Cambridge, UK and New York, USA.
3. Lagaros ND (2020) The environmental and economic impact of structural optimization. *Struct Multidiscip O* 49:1047-1066
4. Mergos PE (2018a) Contribution to sustainable seismic design of reinforced concrete members through embodied CO2 emissions optimization. *Struct Concrete* 19:454-462.
5. Mergos PE (2018b) Seismic design of reinforced concrete frames for minimum embodied CO2 emissions. *Energ Buildings* 162:177-186
6. Sarma KC, Adeli H (1997) Cost optimization of concrete structures. *J Struct Eng* 124:570-578
7. Lagaros ND (2014) A general purpose real-world structural design optimization computing platform. *Struct Multidiscip O* 49:1047-1066
8. Zakian P, Kaveh A (2023) Seismic design optimization of engineering structures: a comprehensive review. *Acta Mechanica* 234: 1305-1330.
9. Yeo D, Gabbai R (2011) Sustainable design of reinforced concrete structures through embodied energy optimization. *Energ Buildings* 43:2028-2033
10. Medeiros G, Kripka M. (2014) Optimization of reinforced concrete columns according to different environmental impact assessment parameters. *Eng Struct* 59:185-194
11. Kayabekir AE, Bekdaş G, Nigdeli SM (2021) Optimum design of reinforced concrete T-beam considering environmental factors via flower pollination algorithm. *Int J Appl Sci Eng* 13:166-178
12. Paya-Zaforteza I, Yepes V, Gonzalez-Vidoso F (2008) Hospitaler A. Multiobjective optimization of concrete frames by simulated annealing. *Comput-Aided Civ Inf* 23:596-610
13. Kaveh A, Sabzi O (2011) A comparative study of two metheuristic algorithms for optimal design of planar RC frames. *Int J Civ Eng* 9: 193-206
14. Akin A, Saka MP (2015) Harmony search algorithm based optimum detailed design of reinforced concrete plane frames subject to ACI 318-05 provisions. *Comput Struct* 147:75-95
15. Mergos PE (2018c) Efficient optimum seismic design of reinforced concrete frames with nonlinear structural analysis procedures. *Struct Multidiscip O* 58:2565-2581
16. Rakici E, Bekdaş G, Nigdeli SM (2020) Optimal cost design of single-story reinforced concrete frames using Jaya algorithm. *CHSA 2020: Proceedings of 6th International Conference on Harmony Search, Soft Computing and Applications* pp 179-186
17. Kaveh A, Izadifard RA, Mottaghi L (2020) Optimal design of planar RC frames considering CO2 emissions using ECBO, EVPS and PSO metaheuristic algorithms. *J Build Eng* 28: 101014
18. Fadaee MJ, Grierson DE (1996) Design optimization of 3D reinforced concrete structures. *Struct. Optimization* 12:127-134
19. Balling RJ, Yao X (1997) Optimization of reinforced concrete frames. *J. Struct. Eng ASCE* 123:193-202
20. Sahab MG, Ashour AF, Toropov VV (2005) Cost optimization of reinforced concrete flat slab buildings. *Eng Struct* 27:313-322
21. Govindaraj V, Ramasany JV (2007) Optimum detailed design of reinforced concrete frames using genetic algorithms. *Eng Optimiz* 39:471-494
22. Sharafi P, Muhammad NS, Hadi M (2012) Heuristic approach for optimum cost and layout design of 3D reinforced concrete frames. *J Struct Eng* 138:853-863
23. Kaveh A, Behnam AF (2013) Design optimization of reinforced concrete 3D structures considering frequency constraints via a charged system search. *Sci Ira Trans A* 20:387-396
24. Esfandiari MJ, Urgessa GS, Sheikholarefin S, Dehghan Manshadi SH (2018) Optimum design of 3D reinforced concrete frames using the DMPSO algorithm. *Adv Eng Softw* 115:149-160
25. Dehnavipour H, Mehrabani M, Fakhriyat A, Jakubczyk-Galczyńska A (2019) Optimization-based design of 3D reinforced concrete structures. *Journal of soft computing in civil engineering* 3:95-106
26. Martins A, Simões L, Negrão J, Lopes A (2020) Sensitivity analysis and optimum design of reinforced concrete frames according to Eurocode 2. *Eng Optimiz* 52:2011-2032
27. Mergos PE (2021) Optimum design of 3D reinforced concrete building frames with the flower pollination algorithm. *J Build Eng* 44:102935
28. Mergos PE (2022) Surrogate-based optimum design of 3D reinforced concrete building frames to Eurocodes. *Developments in the Built Environment* 11:100079
29. Bartz-Beielstein T, Doerr C, *et al.* (2020) Benchmarking in optimization: Best practice and open issues. *arXiv:2007.03488v2*
30. Rosenbrock H (1960). An Automatic Method for Finding the Greatest or Least Value of a Function. *The Computer Journal* 3:175-184
31. Rastrigin LA (1974) Systems of extremal control. Mir, Moscow.

32. Tang K, Li X, Suganthan PN, Yang Z, Weise T (2010). Benchmark Functions for the CEC'2010 special session and competition on large-scale global optimization. Technical report, available online at: <https://titan.csit.rmit.edu.au/~e46507/publications/lsgo-cec10.pdf>
33. Liang J, Qu B, Suganthan P, Hernandez-Daz AG (2013) Problem definitions and evaluation criteria for the CEC2013 special session on real-parameter optimization. Computational Intelligence Laboratory, Zhengzhou University, Zhengzhou China and Nanyang Technological University, Singapore, Technical Report 20121
34. Jamil M, Yang XS (2013) A literature survey of benchmarks functions for global optimization problems. *International journal of mathematical modelling and numerical optimisation* 4:150-194.
35. Mergos PE, Yang XS (2021) Flower pollination algorithm parameters tuning. *Soft computing* 25:14429-14447
36. Kumar A, Wu G, Ali M, Mallipeddi R, Suganthan PN, Das S (2020) A test-suite of non-convex constrained optimization problems from the real-world and some baseline results. *Swarm and evolutionary computation* 56: 100693.
37. Goh SK, Tan KC, Al-Mamun A, Abbass HA (2015) Evolutionary big optimization of signals. In 2015 IEEE Congress on Evolutionary Computation, IEEE.
38. Gallagher M (2016) Towards improved benchmarking of black-box optimization algorithms using clustering problems. *Soft Computing* 20: 3835-3849
39. Volz V, Naujoks B, Kerschke P, Tusar T (2019) Single- and multi-objective optimization game-benchmarks for evolutionary algorithms. In *Proceedings of the 2019 Genetic and Evolutionary Computation Conference*, 647-655.
40. Haftka R (2016) Requirements for papers focusing on new algorithms or improved global optimization algorithms. *Structural and Multidisciplinary Optimization* 54:1-1
41. CEN (2000) Eurocode 2: Design of concrete structures. Part 1-1: General rules and rules for buildings, Brussels: European Standard EN 1992-1-1
42. CEN (2004) Eurocode 8: Design of structures for earthquake resistance. Part 1: General rules, seismic actions and rules for buildings, Brussels: European Standard EN 1990-1.
43. CEN (2002) Eurocode 0: Basis of Structural Design. Brussels: European Standard EN 1992:2002
44. CSI (2022) <https://www.csiamerica.com/products/sap2000>
45. MathWorks (2022a) https://uk.mathworks.com/products/matlab.html?s_tid=hp_products_matlab
46. CSI (2016) Concrete frame design manual: Eurocode 2-2004 with Eurocode 8-2004 for SAP2000. ISO SAP091415M29 Rev. 1, USA.
47. Moss R, Brooker O (2006) How to design concrete structures using Eurocode 2: Beams. The Concrete Centre, Surrey, UK
48. MathWorks (2022b) MATLAB R2022b – Global Optimization Toolbox. Natick, MA, USA
49. Holland JH (1975) Adaptation in natural and artificial systems. An introductory analysis with application to biology, control and artificial intelligence. University of Michigan Press, Ann Arbor, MI
50. Yang XS (2012) Flower pollination algorithm for global optimization. *Unconven Comput Nat Comput* 7445:240-249
51. Kennedy J (2001) Particle swarm optimization. *Encyclopedia of Machine Learning*, Springer:760-766
52. Kirkpatrick S, Gelatt CD, Vecchi MP (1983) Optimization by simulated annealing. *Science* 220:671-680
53. Deb K, Pratap A, Agarwal S, Meyarivan T (2002) A fast and elitist multi-objective genetic algorithm: NSGA-II. *IEEE Trans Evol Comput* 6:182-197